BMC Pediatrics

RESEARCH

Open Access

Using machine learning models based on cardiac magnetic resonance parameters to predict the prognostic in children with myocarditis

Dongliang Hu[1,2†], Manman Cui[1†], Xueke Zhang[1], Yuanyuan Wu[1], Yan Liu[1], Duchang Zhai[1], Wanliang Guo[2], Shenghong Ju[3], Guohua Fan[1] and Wu Cai[1*]

Abstract

Objective To develop machine learning (ML) models incorporating explanatory cardiac magnetic resonance (CMR) parameters for predicting the prognosis of myocarditis in pediatric patients.

Materials and methods 77 patients with pediatric myocarditis diagnosed clinically between January 2020 and December 2023 were enrolled retrospectively. All patients were examined by ultrasound, electrocardiogram (ECG), serum biomarkers on admission, and CMR scan to obtain 16 explanatory CMR parameters. All patients underwent follow-up echocardiography and CMR. Patients were divided into two groups according to the occurrence of adverse cardiac events (ACE) during follow-up: the poor prognosis group ($n=23$) and the good prognosis group ($n=54$). Four models were established, including logistic regression (LR), random forest (RF), support vector machine classifier (SVC), and extreme gradient boosting (XGBoost) model. The performance of each model was evaluated by the area under the receiver operating characteristic curve (AUC). Model interpretation was generated by Shapley additive interpretation (Shap).

Results Among the four models, the three most important features were late gadolinium enhancement (LGE), left ventricular ejection fraction (LVEF), and SAXPeak Global Circumferential Strain (SAXGCS). In addition, LGE, LVEF, SAXGCS, and LAXPeak Global Longitudinal Strain (LAXGLS) were selected as the key predictors for all four models. Four interpretable CMR parameters were extracted, among which the LR model had the best prediction performance. The AUC, sensitivity, and specificity were 0.893, 0.820, and 0.944, respectively. The findings indicate that the presence of LGE on CMR imaging, along with reductions in LVEF, SAXGCS, and LAXGLS, are predictive of poor prognosis in patients with acute myocarditis.

†Dongliang Hu and Manman Cui contributed equally to this work.

*Correspondence:
Wu Cai
xwg608@126.com

Full list of author information is available at the end of the article

Conclusion ML models, particularly the LR model, demonstrate the potential to predict the prognosis of children with myocarditis. These findings provide valuable insights for cardiologists, supporting more informed clinical decision-making and potentially enhancing patient outcomes in pediatric myocarditis cases.

Keywords Myocarditis, Magnetic resonance imaging, Major cardiovascular adverse events, Machine learning

Introduction

Myocarditis is an acute or chronic inflammatory disease of the myocardium that can be caused by infectious pathogens such as viruses, bacteria, fungi and Chlamydia, as well as by toxic and hypersensitivity reactions [1]. The pathological features include degeneration, necrosis and fibrosis of myocardial cells, which may eventually cause severe structural and functional impairment of the heart muscle [1]. The increase in the number of patients with myocarditis has been reported after the COVID-19 pandemic. In addition, COVID-19 vaccine-related myocarditis is a condition in which a person experiences localized or diffuse inflammatory changes in the heart muscle as the main manifestation after receiving the COVID-19 vaccine [2]. In the United States, there have been nearly 1,300 reports of myocarditis related to vaccination among over 350 million doses administered, and there have been fatal cases of vaccine-related myocarditis in the United States, Israel, and other places [2]. Acute myocarditis comprises a broad clinical spectrum, from subclinical disease to severe heart failure, and is a major cause of sudden death in young adults. Pathologically, it is characterized by inflammatory cell infiltration of the myocardium with evidence of myocyte necrosis that is not characteristic of an ischemic etiology. Myocarditis can be caused by infections, immune-mediated injury, and toxins (such as anthracyclines) [1].

MRI has high spatial fidelity, good repeatability, strong diagnostic consistency, functional imaging, and quantitative analysis. Cardiovascular magnetic resonance imaging (CMR) is a recognized technique for diagnosing cardiovascular diseases, which is highly specific, sensitive, and non-invasive. It is a very practical method when the clinical diagnosis is unclear, and the specificity of auxiliary examination is not robust. Based on the results of multiple studies [3, 4], the sensitivity of CMR in diagnosing myocarditis is 60–85%, the specificity is 68–90%, and the diagnostic accuracy is close to 80%, which is in line with the diagnostic patterns of myocarditis. It can accurately evaluate the shape and function of the heart, quantify myocardial strain and perfusion function, detect the existence of myocardial edema and fibrosis, and provide important reference value for the diagnosis and prognosis of myocarditis [5–7]. Late gadolinium enhancement (LGE) is a marker of myocardial fibrosis and can reflect the existence of myocardial fibrosis [8, 9]. Related studies have confirmed the value of LGE in predicting the prognosis of patients with myocarditis [10–13].

In recent years, imaging techniques have been widely used for clinical risk stratification and prognosis prediction of diseases. CMR imaging is an effective tool for predicting cardiac events [14–16]. However, the traditional features visually extracted from images cannot be fully explained by medical knowledge. In this study, the detailed parameters of cardiac function, strain and tissue characteristics were further extracted by CMR analysis software, and an interpretable prediction model was constructed. Most of the models established by interpretable CMR parameters to predict the prognosis of myocarditis are concentrated in adult patients with myocarditis, while few studies have evaluated the prognosis of children with myocarditis [10–13]. Therefore, this study aimed to explore the feasibility of the machine-learning model based on interpretable CMR parameters for predicting the prognosis of children with myocarditis.

Materials and methods

Patient enrollment

The study was performed with approvals from the Second Affiliated Hospital of Soochow University institutional board and ethical committee, and was carried out in strict accordance with the relevant guidelines for the acquisition and use of human information and specimens, and the Declaration of Helsinki. Informed consent was waived because of the retrospective nature of the study. Patients who underwent CMR examinations ($n = 93$) between January 2020 and December 2023 were retrospectively enrolled. Patients without follow-up data ($n = 7$), with unqualified CMR data ($n = 4$), and with congenital heart disease ($n = 5$) were excluded. Ultimately, 77 patients were enrolled in the study.

Inclusion criteria and exclusion criteria

The inclusion criteria were as follows: (1) age < 18 years; (2) in accordance with the diagnostic guidelines for American Heart Association (AHA) myocarditis in children in 2022 [17]; (3) had undergone selective angiography excluding coronary artery disease; (4) good quality of MRI images.

The exclusion criteria were as follows: (1) patients without follow-up evaluation; (2) patients with unqualified CMR data (unqualified CMR data are defined as CMR data with significant motion artifacts, missing key sequences [such as LGE], insufficient image fidelity, or inability to accurately measure myocardial fibrosis and

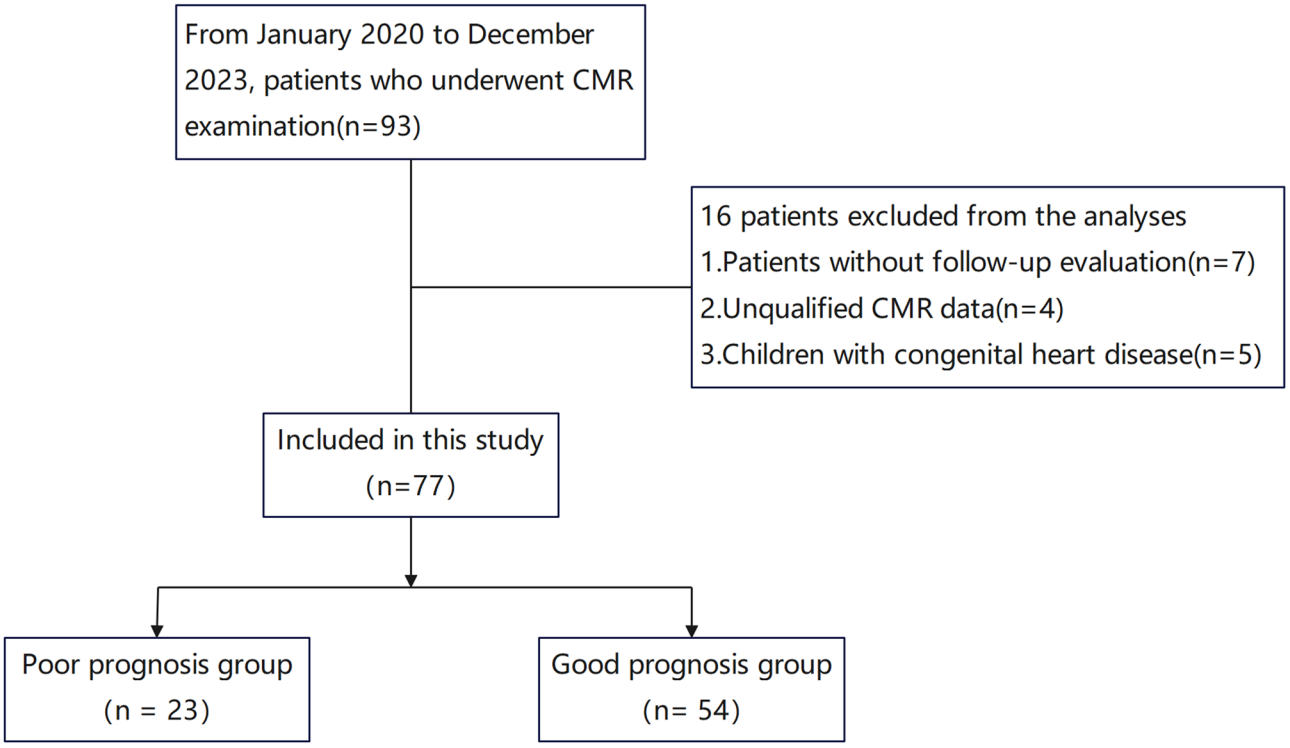

Fig. 1 Flowchart of patient enrollment

Table 1 CMR scanning sequences and parameters

	Discovery750W, GE (*n* = 12)			IngeniaCX, Philips (*n* = 65)		
	Heart film	T2WI	LGE	Heart film	T2WI	LGE
Flip angle (°)	45	107	15	45	90	25
Repetition time (ms)	3.42	1100	6.69	2.84	1200	4.53
Echo time (ms)	1.54	69	3.16	1.42	75	2.20
Slice thickness(mm)	6	6	6	6	6	6

LGE = Late gadolinium enhancement

cardiac function parameters); (3) patients with congenital heart disease.

Patient characteristics

The flowchart of patient enrollment is shown in Fig. 1. The 77 children included 44 males and 33 females aged 0–16 years, with an average age of 9.4 ± 4.2 years. According to the previous description of myocarditis [18–23], it includes the following manifestations: (1) symptoms and signs of acute myocarditis within 2 weeks of admission, such as fever, prodromal symptoms of the virus, chest tightness, chest pain, dyspnea, palpitation, headache or syncope, a small number of patients have abdominal pain and diarrhea; (2) evidence of structural or functional abnormalities on echocardiography or CMR; (3) abnormal electrocardiogram; (4) increased serum biomarkers, which include cardiac troponin T (cTnT), creatine kinase MB (CK-MB), myoglobin (MYO), and B-type natriuretic peptide (BNP). The mean follow-up duration was 2.8 ± 2.5 years. Patients were divided into a poor prognosis group (*n* = 23) or a good prognosis group (*n* = 54) according to the occurrence of adverse cardiac events (ACE) during follow-up. ACE was defined as follows: (1) death or heart transplantation; (2) re-admitted to hospital for heart failure; (3) persistent ventricular arrhythmias; (4) treatment with implantable cardioverter-defibrillator; (5) follow-up MRI or echocardiography showing left ventricular dysfunction and dilated cardiomyopathy. One of these criteria could be defined.

Method

Scanning methods and parameters

CMR was performed via 3.0T MRI (Discovery750W, GE Healthcare, Boston, USA [65 patients] and IngeniaCX, Philips Healthcare, Best, Netherlands [12 patients]) and triggered via retrospective electrocardiographic (ECG) gating, and included the following sequences (Table 1): (1) heart film: the balanced steady-state free precession

sequence was used for scanning; (2) T2WI: three inversion black blood T2WI sequences were used for scanning; (3) LGE: after first pass myocardial perfusion imaging, 0.2mmol/kg gadolinium meglumine (6.654 g/15 ml, Hengrui Pharmaceuticals, Shanghai, China) was injected, and a phase sensitive inversion recovery sequence was used for scanning after 10 min. All the scanning sequences capture 3 long-axis images (four-chamber, two-chamber, and three-chamber images). Film sequence and LGE were used to capture all short-axis images from base to apical. T2WI were used to capture three short-axis images: basal, middle, and apical images.

Image analysis

All the CMR data were post-processed by commercial software CVI42Client (Circle Cardiovascular Imaging, Calgary, Canada). The myocardium was segmented layer by layer in the short-axis view. The epicardium and endocardium contours were delineated using a semi-automatic method. This process combines region-growing, active contour models, and manual adjustments. By removing interference from papillary muscles and the blood pool, and applying smoothing, accurate segmentation results were achieved [3]. This segmentation method is endorsed by the Society for Cardiovascular Magnetic Resonance. According to the AHA segmented method, the myocardium was divided into 17 segments. The generated quantitative CMR parameters had three parts: (1) 11 quantitative parameters related to cardiac function, which including the ejection fraction (EF), end-diastolic volume (EDV), end-systolic volume (ESV), and so on, automatically generated by processing the short-axis film sequence with CVI short-axis 3D module, (2) three layers of short-axis LGE which relate to myocardial fibrosis, generated by processing the LGE sequence with the CVI organization feature module. LGE parameters measure the intensity of myocardial enhancement globally. It was included in the model as categorical variables (presence/absence of enhancement). Segments with a signal intensity ratio above a predefined threshold (typically > 5 standard deviations above the mean signal intensity of normal myocardium) were considered enhanced. (Fig. 2). (3) four left ventricular (LV) strain-related quantitative parameters, automatically generated by processing long-axis and short-axis cinematographic sequences with the CVI tissue tracking module (Fig. 3). These strains include the SAXPeak Global Circumferential Strain (SAXGCS), SAXPeak Global Radial Strain (SAXGRS), LAXPeak Global Longitudinal Strain (LAXGLS) and LAXPeak Global Radial Strain (LAXGRS). A total of 16 CMR parameters are obtained. To evaluate consistency of each feature, we randomly selected 30 cases for repeated segmentation. In this feature subgroup, the viewer 1 repeated the image segmentation twice, and the viewer 2 divided the image independently to evaluate the reproducibility within and between observers. According to the quantitative reproducibility of the intra-group correlation coefficient (ICC), ICC > 0.90 indicates high consistency.

Prediction models and evaluation

To predict the prognosis of children with myocarditis, we explored four machine learning (ML) algorithms: Logistic Regression (LR) for binary classification tasks, Random Forest (RF) as an ensemble learning method based on decision trees, Support Vector Classifier (SVC) as a kernel-based classification method, and Extreme Gradient Boosting (XGBoost) for its scalable and efficient implementation of gradient boosting on decision trees. All the models were developed in Python (version 3.9.12). The LR, RF, SVC, and XGBoost models are implemented using the Python scikit-learn package. Since this is a single-center study, the models obtained from the random segmentation of training and test data may not be generalized. Therefore, ten cross-validations were used to evaluate the performance of the model. Seven performance indicators were recorded in each iteration, including the area under the curve (AUC), sensitivity, specificity, accuracy, F1 score, positive predictive value (PPV) and negative predictive value (NPV). The model was compared in each dataset using average AUC values from ten iterations. The best-performing ML model was selected and measured by its average AUC value. To further validate the models' performance, we conducted bootstrapping analysis to assess their robustness across different metrics. Bootstrapping was performed with 1,000 resampling iterations. In each iteration, 80% of the original dataset was randomly sampled with replacement to form the training subset, while the remaining 20% was retained as the hold-out validation subset. All machine learning models were retrained on the resampled training data, and their performance was evaluated on the corresponding validation subset. The AUC was computed for each iteration. Final model performance metrics (mean ± standard deviation) and 95% confidence intervals (CIs) were derived using the percentile method. Shapley additive interpretation (Shap) was used to explain the prediction of the ML model and to select the top ten features that have the most significant impact on the prediction.

Statistical analysis

The patients were divided into two groups, the good prognosis group and the poor prognosis group, and the variables were compared between the two groups. Independent sample t-test were used for continuous variables with a normal distribution. Variables with non-normal distribution were analyzed via the Mann-Whitney U test. The chi-square ($\chi 2$) test or Fisher's exact test was used to categorical variables. Pearson's chi-square test was

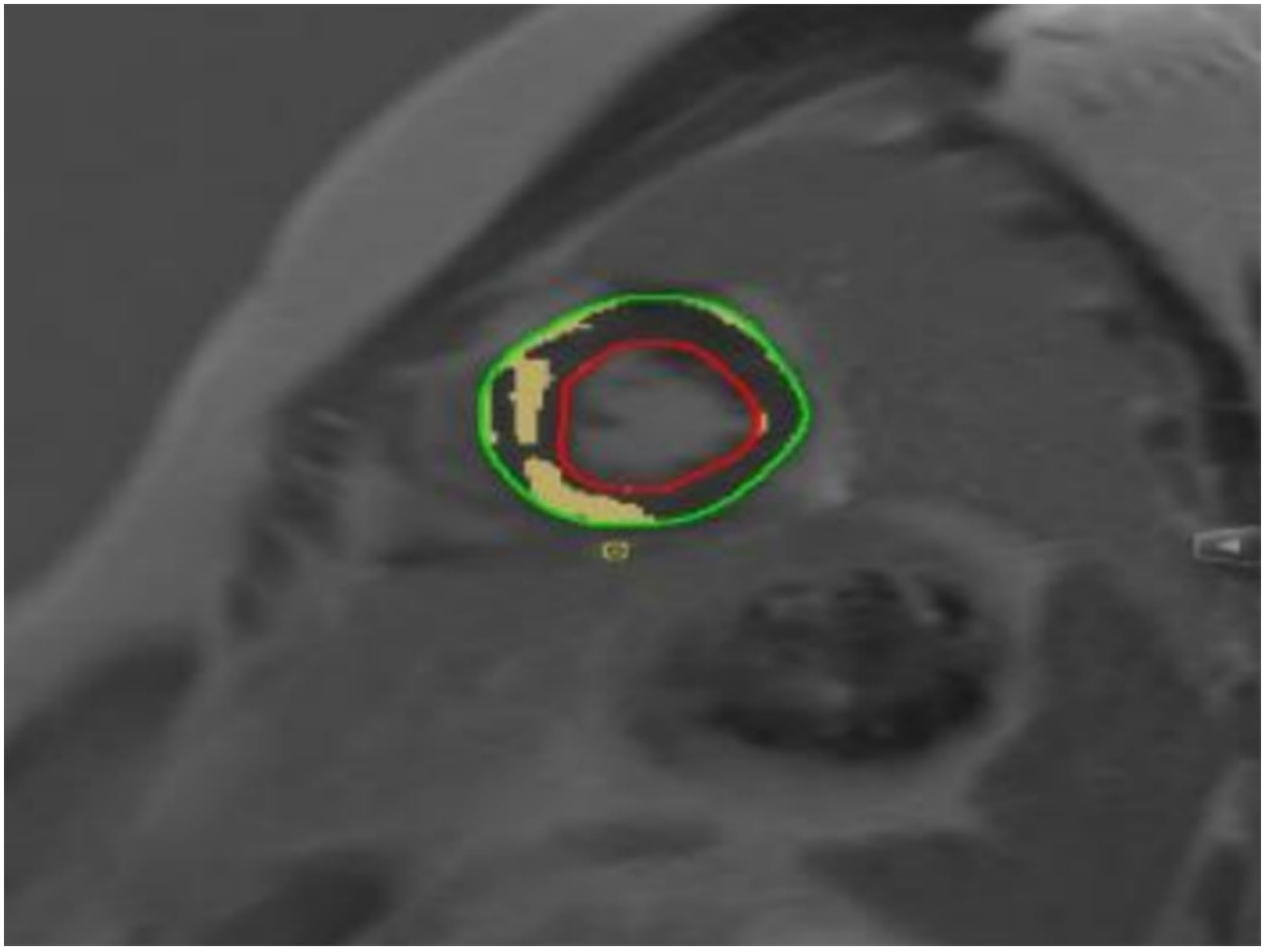

Fig. 2 Late gadolinium-enhanced images of the left ventricle short axis; red: endocardial line of the left ventricle; green: left ventricular epicardial line; yellow: delayed reinforcement area (the myocardial gray threshold is 5 standard deviations greater than the average signal strength of normal myocardium to determine late enhancement)

systematically applied when all expected cell frequencies exceeded 5 with a total sample size ≥ 40, while Fisher's exact test was preferentially employed under conditions where any expected cell frequency fell below 5 or the total sample size was < 40. All the statistical analyses used Python (version 3.9.12) and R software (version 4.2.1), and $P < 0.05$ was considered significant.

Results

Cohort characteristics:77 patients with clinical features were divided into two groups. The most common symptoms were chest pain ($n = 47$) and fever ($n = 32$), followed by abdominal pain ($n = 25$) and respiratory symptoms ($n = 17$). A few patients developed dizziness and headache ($n = 14$). 7 patients had a recent history of novel coronavirus infection (within 3 months). Most patients had abnormal ECG (77.9%), and 26 patients had ventricular tachycardia (33.8%). The elevation of the ST-segment was the second common (32.5%), followed by depression of the ST-segment (11.7%). 7 patients underwent Endomyocardial biopsy, of whom 6 were diagnosed with acute myocarditis. In addition, 6 patients had pericardial effusion. There was no significant difference in infection type, clinical manifestation, heart rate, body mass index (BMI), serum biomarkers and ultrasonography result between the good and poor prognosis groups (Table 2). At the end of the follow-up, all patients survived, and no patients received heart transplantation.

CMR results: Patients with myocarditis were examined by cardiovascular MRI in the hospital within 4.5 ± 7.5 days after onset. Univariate analysis revealed significant differences in LGE, left ventricular ejection fraction (LVEF), SAXGCS, LAXGLS, the LV cardiac index (LVCI), LVEF is the percentage of ejected volume from the LV during systole relative to end-diastolic volume. LVMASS V/B (Value/Body surface area), right ventricular ejection fraction (RVEF), and ST elevation between the two groups, all patients with an average LVEF of 64.0%. Compared with adult myocarditis patients, LVEF damage was less common in children. The average RVEF is 57.9%.

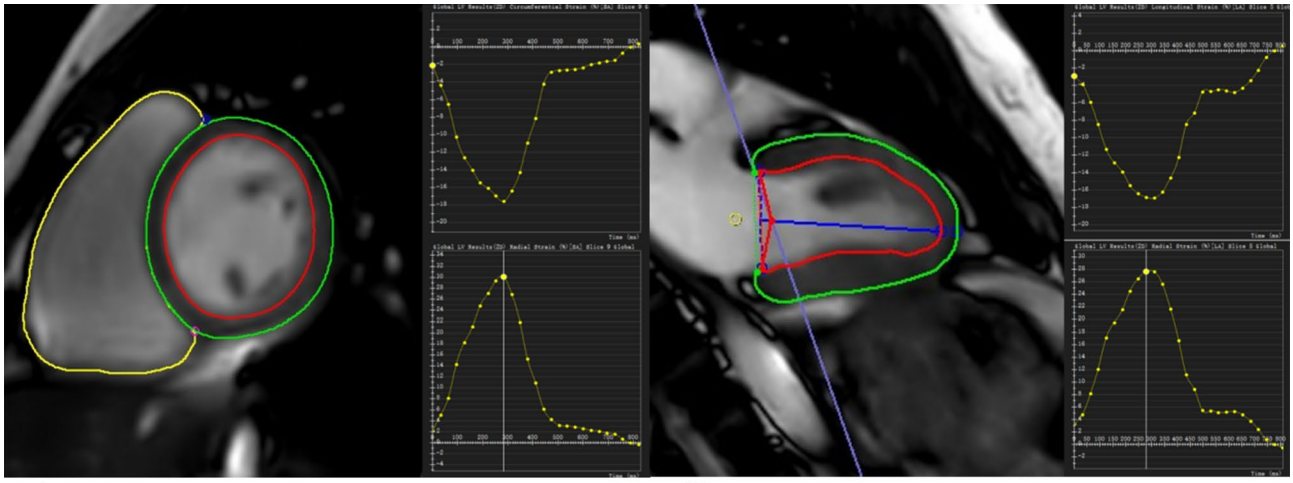

Fig. 3 Myocardial strain measurement via the feature tracking method in an 8-year-old female patient with acute myocarditis. After the endocardial and epicardial borders of the LV were traced semi-automatically, The software (CVI42) automatically tracked the endocardial and epicardial borders across frames during the cardiac cycle. SAXGCS and SAXGRS measurements (**A**) were obtained via mid-ventricular level short-axis cine views. LAXGRS and LAXGCS measurements (**B**) were obtained from 2-chamber long-axis view. SAXGCS = SAXPeak Global Circumferential Strain measured from short-axis cine views, LAXGLS = LAXPeak Global Longitudinal Strain measured from long-axis cine views, LAXGRS = LAXPeak Global Radial Strain measured from long-axis cine views, SAXGRS = SAXPeak Global Radial Strain measured from short-axis cine views, LV = left ventricular

39% of LGE cases were located in the inferior lateral wall, and 42% were in the middle interventricular septum. There was no significant difference in other cardiac function parameters, such as the left ventricular end-diastolic volume (LVEDV) V/B or right ventricular cardiac index (RVCI), between the patient group and the control group (Table 2).

Predictive performance of the ML models

All 32 features are included in the model input, including 16 clinical features such as demographics, clinical symptoms of myocarditis, laboratory tests, ECG results, and 16 CMR parameters (Table 2). Among the ML models considered, the LR model (AUC = 0.893) is superior to the RF (AUC = 0.884), SVC (AUC = 0.880), and XGBOOST (AUC = 0.840) models (Fig. 4; Table 3). The Youden index was used to optimize the index and decision threshold of each model. Under this optimization threshold, the sensitivity and specificity of the LR model are 82.0% and 94.4%, respectively. Bootstrap validation with 1,000 iterations further corroborated the LR model's robustness, demonstrating consistent performance superiority (AUC = 0.895) over RF (AUC = 0.865), SVC (AUC = 0.862), and XGBoost (AUC = 0.828). The receiver operating characteristic (ROC) curves for all models, with translucent shading representing 95% CIs superimposed, are available in the Supplementary Material 2.

Model interpretation

Shap software was used to explain the prediction of four ML models (LR, SVC, RF, and XGBOOST). Figure 5 shows the functional importance ranking based on the mean| Shap Value|, with the top ten features filtered out for each model. Among all the models, LGE, LVEF, SAXGCS and LAXGLS were the four most important features. Figure 6 shows the positive or negative contributions of the top 10 features to the prognosis of myocarditis in children. In Fig. 6, each point represents a data sample, and the color indicates whether the observation of the feature itself is greater (redder) or lower (bluer). The features, including LGE, reduced SAXGCS, impaired LAXGLS, decreased LVEF, and ST-segment elevation on ECG, demonstrate a positive correlation with ACE.

Discussion

In this study, the clinical and CMR data of children with myocarditis were involved to predict the prognosis via ML algorithm, including LR, RF, SVC, and XGBoost models. The prediction effect of the LR model was the best, and the AUC value was the highest. The four ML models screened out important prognostic factors, including LGE, LVEF, SAXGCS, LAXGLS, and ECG ST-segment elevation. Predicting the occurrence of ACE in children with myocarditis is important for early clinical treatment. This study chose LR and nonlinear models (including SVC, RF, and XGBoost) to ensure the reliability and robustness of our results. This approach helps to mitigate potential biases or inaccuracies that might arise from relying on a single model, thereby providing a more balanced and comprehensive evaluation of the data. In the ROC analysis, the LR model had the highest

Table 2 Patient characteristics

	ALL	Good prognosis	Poor prognosis	*P*-value
Age	9.36 ± 4.12	9.32 ± 4.04	9.44 ± 4.56	0.907
Female	41	30	11	0.540
Chest pain	47	35	12	0.304
Fever	32	23	9	0.781
Abdominal pain	25	18	7	0.807
Respiratory symptoms	17	12	5	0.963
Headache	14	8	6	0.246
Type of infection	34	20	14	0.055
CRP	3.74(0.89, 13.2)	3.45(0.91,16.80)	4.30(0.10,10.25)	0.269
cTNT	114.60(48.13,446.80)	110.75(41.01,393.10)	134.5(68.84,490.60)	0.302
MYO	30.04(16.0,94.0)	30.07(16.5,87.45)	28.01(17.0,136.56)	0.800
BNP	254.0(90.0,626.2)	206.80(72.60,445.45)	456.0(184.9,1397.0)	0.264
CKMB	9.80(2.70,20.12)	10.35(3.15,21.66)	8.9(2.55,19.15)	0.328
ST elevation	25	10	15	< 0.001
ST depression	9	6	3	0.812
Ventricular tachycardia	26	16	10	0.245
BMI	18.21 ± 3.99	18.49 ± 4.05	17.56 ± 3.86	0.354
BSA	1.16 ± 0.43	1.18 ± 0.44	1.11 ± 0.40	0.511
LVEDV V/B	76.18 ± 14.71	74.07 ± 12.41	81.12 ± 18.44	0.054
LVESV V/B	25.32(21.76,31.32)	25.13(21.85,31.12)	27.01(22.14,31.59)	0.236
LVEF	64.0(55.0, 68.0)	66.0(62.0,69.0)	49.0(46.0,59.0)	< 0.001
LVCI	4.44 ± 0.94	4.25 ± 0.88	4.89 ± 0.95	0.005
LVMASS V/B	45.70(40.14,52.18)	44.89(39.59,48.74)	49.72(43.27,61.62)	0.012
RVEDV V/B	69.12 ± 17.05	69.45 ± 15.42	68.35 ± 20.75	0.796
RVESV V/B	28.89 ± 7.66	28.84 ± 6.78	29.01 ± 9.57	0.929
RVEF	57.857 ± 5.33	58.74 ± 4.24	55.78 ± 6.97	0.025
RVCI	3.44 ± 1.09	3.43 ± 0.97	3.47 ± 1.35	0.861
SAXPeak Global Circumferential strain	0.17(0.11,0.20)	0.18(0.16,0.2)	0.10(0.05,0.15)	< 0.001
SAXPeak Global Radial strain	0.32 ± 0.08	0.32 ± 0.08	0.31 ± 0.09	0.516
LAXPeak Global Longitudinal strain	0.13 ± 0.04	0.14 ± 0.04	0.09 ± 0.04	< 0.001
LAXPeak Global Radial strain	0.22 ± 0.09	0.22 ± 0.09	0.20 ± 0.08	0.323
LGE	19	2	17	< 0.001

The data are presented as n (%) or mean ± SD. CRP = C-reactive protein cTNT = cardiac troponinT, MYO = myoglobin, BNP = b-type natriuretic peptide, CK-MB = creatine kinase MB, BMI = body mass index, BSA = body surface area, LV = left ventricular, EDV = end-diastolic volume, ESV = end-systolic volume, EF = ejection fraction, CI = cardiac index, RV = right ventricular, LGE = late gadolinium enhancement, V/B = Value/Body surface area

AUC value of 0.893 and outperformed the LR, SVC, and XGBoost models.

LGE is a marker of myocardial fibrosis and can reflect the existence of myocardial fibrosis [8, 9]. Related studies have confirmed the value of LGE in predicting the prognosis of patients with myocarditis [10–13]. It is reported that the presence of LGE is an independent predictor of poor prognosis, defined as heart transplantation, the need for extracorporeal membrane oxygenation or a ventricular assist device, and death [24, 25], which is consistent with our results. In addition, a recent long-term prognosis study in patients with acute myocarditis revealed that New York Heart Association functional grade II and a larger range of LGE were independent predictors of long-term major adverse cardiovascular events [26]. However, Aquaro et al. [10, 11]found that LGE in patients with myocarditis mainly existed in the subepicardium of the inferior lateral wall (41%) and anterior middle septum (36%). In contrast, patients with LGE located in the anterior middle septum had a poor prognosis, similar to the results of our study. In our study, LGE was detected among 24.7% of the patients, of which approximately 39% were in the inferior lateral wall and 42% in the middle interventricular septum. Therefore, we believe that the location of LGE has greater prognostic significance than the range of LGE, which is consistent with previous studies [10, 11]. This conclusion has high clinical value and can be used to guide the clinical prediction of myocarditis and to take preventive measures as soon as possible.

LVEF refers to the percentage of left ventricular end-systolic ejection volume to LVEDV, which can reflect the degree of impaired cardiac function. Some studies have shown that the value of LVEF is lower in patients who

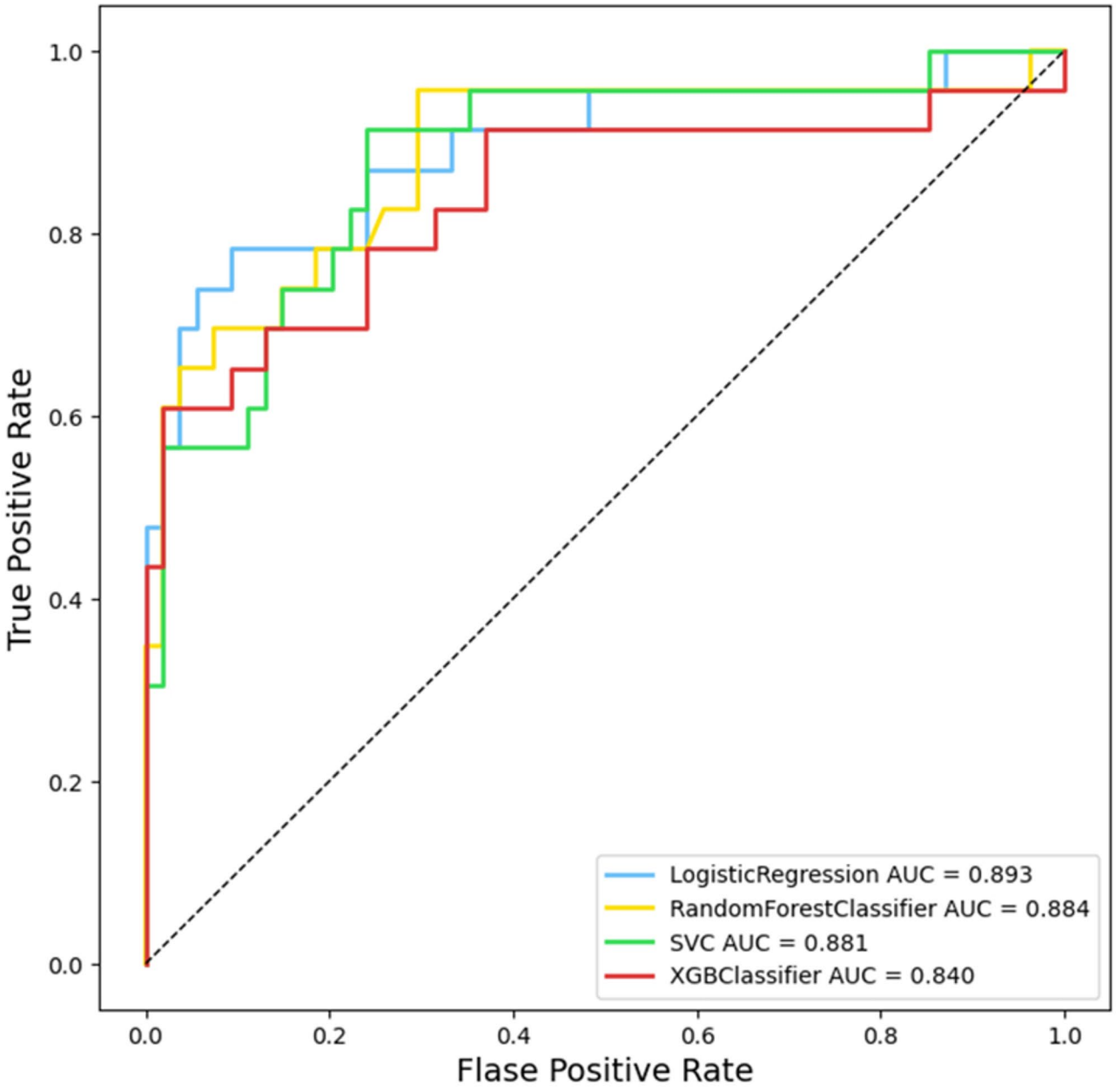

Fig. 4 Areas under the receiver operating characteristic curve (AUC) for all four machine learning models [logistic regression (LR), random forest (RF), support vector machine classifier (SVC), and extreme gradient boosting (XGBoost)]

died from myocarditis [27]. Patients with an LVEF < 0.30 have a poor prognosis and a significantly increased risk of mechanical circulatory support, death, or heart transplantation ($P < 0.001$) [27]. Cardiac dysfunction can strongly activate the natriuretic peptide system, and increased ventricular load can lead to the release of BNP. Patients with myocarditis with an LVEF < 0.50 had higher levels of BNP [28], and their peak BNP ($P > 10000$ ng/L) was a risk factor for poor prognosis of pediatric myocarditis [25].

Myocardial strain refers to the degree of deformation of a cardiac segment from its original shape (end-diastole) to its maximum length (end-systole) in a specified direction and is expressed in percentage terms of the deformation. Feature tracking cardiovascular magnetic resonance (FT-CMR) imaging can be used to quantitatively evaluate changes in myocardial strain of patients with myocarditis based on conventional CMR films and analyze the degree and difference in myocardial systolic and diastolic function damage, which is highly valuable for the diagnosis and prognosis of myocarditis. According to a

Table 3 Performance of each predictive model

	LR	RF	SVC	XGBoost
Accuracy	0.870	0.857	0.805	0.870
Sensitivity	0.820	0.786	0.736	0.795
Specificity	0.944	0.963	0.907	0.981
AUC	0.893	0.884	0.880	0.840
PPV	0.842	0.875	0.722	0.933
NPV	0.879	0.852	0.831	0.855
F1-score	0.836	0.811	0.751	0.825

Decision thresholds were optimized via the Youden index

LR = logistic regression, RF = random forest, SVC = support vector machine classifier, XGBoost = extreme gradient boosting, AUC = area under the curve, CI = confidence interval, PPV = positive predictive value, NPV = negative predictive value

recent review [29], a decreased GCS, or locally circumferential myocardial dysfunction, represents a response to increased wall stress and reflects local changes in myocardial characteristics, such as fibrosis or ischemia caused by microvascular disease or coronary atherosclerotic heart disease. This increased afterload may lead to progressive myocardial remodeling and the development of dysfunction, leading to a poor prognosis [30]. In addition, there was a significant correlation between the GCS and the LV quality index, which reemphasized the relationship between strain reduction and subclinical heart failure, which may be transformed into symptomatic disease due to poor ventricular remodeling [30, 31]. In addition, studies have shown that the left ventricular strain parameters, especially GLS, are impaired in patients with myocarditis compared with healthy volunteers [32, 33]. GLS is considered to be a strong predictor of major ACE in immune point inhibitor-associated myocarditis [32]. Changes in myocardial strain parameters, especially GLS, are considered to be useful in detecting early changes in cardiac insufficiency [34–36]. Early cardiac dysfunction in most progressive cardiomyopathies leads to a decrease in left ventricular longitudinal mechanics, especially in dilated cardiomyopathy [37]. GLS is an independent predictor of survival in patients with dilated cardiomyopathy [34]. It is speculated that in children with myocarditis, more severe damage to the myocardial short-axis GCS and long-axis GLS strain parameters will increase the risk of left ventricular dysfunction and long-term dilated cardiomyopathy, thus affect the prognosis of patients.

ST-segment elevation is the most common change in the ST-segment in acute myocarditis, but ST-segment depression also occurs. In myocarditis, two ST-segment elevation patterns have been described: pericarditis or the typical mode of myocardial infarction. In a study by Nucifora G et al., total ST-segment elevation in all leads was more significant in patients with larger LGE [38].

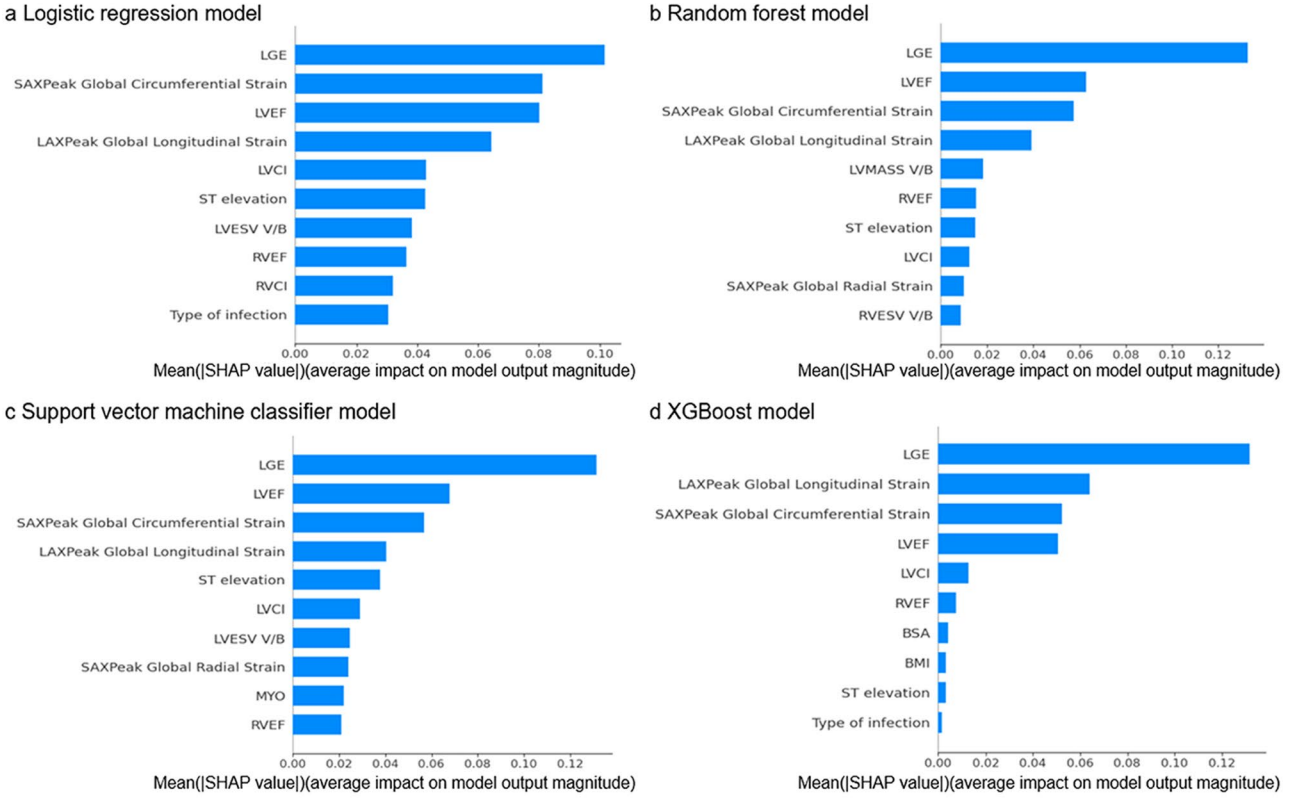

Fig. 5 Importance of the top ten features for each model based on Shapley Additive Explanations (SHAP)

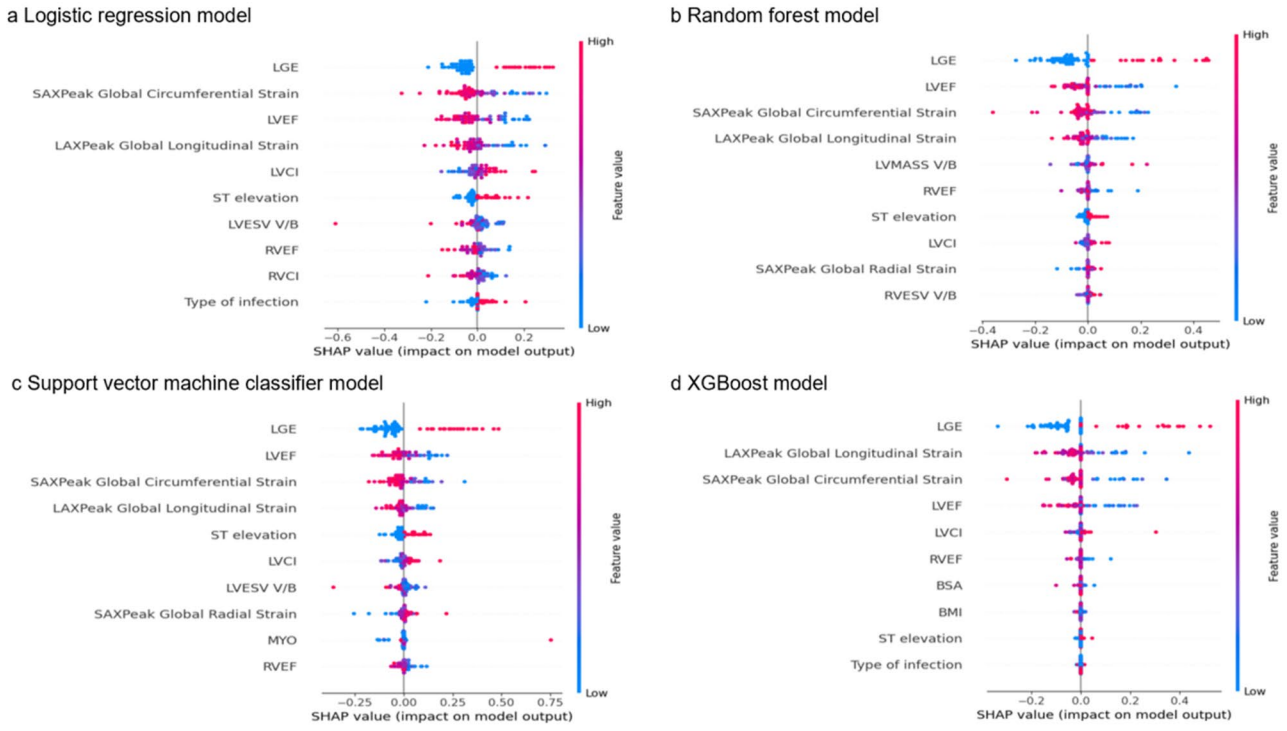

Fig. 6 Shapley Additive Explanations (SHAP) for interpreting the top ten features in each machine learning model

Our model shows that ECG ST-segment elevation is closely related to prognosis in children with myocarditis.

This retrospective study has several limitations. First, the relatively small sample size limits the generalizability of the findings and precludes subgroup analysis. Future studies with larger cohorts and prospective designs are needed to enhance the robustness and persuasiveness of the results. Second, most patients were diagnosed clinically without endocardial biopsy confirmation, which may introduce diagnostic uncertainty. Third, the latest Lake Louise criteria have reduced the diagnostic emphasis on early gadolinium enhancement (EGE), leading to its exclusion from the final analysis. This may affect the comprehensiveness of the imaging assessment. Addressing these limitations in future research could further strengthen the validity and applicability of the findings.

Conclusion

In summary, ML models, particularly the LR model, which are based on clinical and imaging data from pediatric myocarditis patients, can effectively predict the prognosis of children with myocarditis. The optimal ML model (LR) offers early warning capabilities and supports more informed treatment strategies. This study will further investigate laboratory and imaging data related to pediatric myocarditis to refine the models and achieve greater diagnostic accuracy.

Abbreviations

CMR	Cardiovascular magnetic resonance imaging
LGE	Late gadolinium enhancement
AHA	American Heart Association
cTnT	Cardiac troponin T
CK-MB	Creatine kinase MB
MYO	Myoglobin
BNP	B-type natriuretic peptide
ACE	Adverse cardiac events
EF	Ejection fraction
EDV	End-diastolic volume
ESV	End-systolic volume
LV	Left ventricular
SAXGCS	SAXPeak Global Circumferential Strain
SAXGRS	SAXPeak Global Radial Strain
LAXGLS	LAXPeak Global Longitudinal Strain
LAXGRS	LAXPeak Global Radial Strain
ICC	Intra-group correlation coefficient
ML	Machine learning
LR	Logistic regression
RF	Random forest
SVC	Support vector machine classifier
XGBoost	Extreme gradient boosting
AUC	Area under the curve
PPV	Positive predictive value
NPV	Negative predictive value
Cis	Confidence intervals
Shap	Shapley additive interpretation
BMI	Body mass index
LVEF	Left ventricular ejection fraction
RVEF	Right ventricular ejection fraction
LVEDV	Left ventricular end-diastolic volume
V/B	Value/Body surface area
RVCI	Right ventricular cardiac index
ROC	Receiver operating characteristic
BNP	B-type natriuretic peptide
FT-CMR	Feature tracking cardiovascular magnetic resonance

Supplementary Information

The online version contains supplementary material available at https://doi.org/10.1186/s12887-025-05753-y.

Supplementary Material 1

Supplementary Material 2

Acknowledgements
None.

Author contributions
Dongliang Hu and Manman Cui raised ideas, Xueke Zhang and Yuanyuan Wu collected the data, Yan Liu and Duchang Zhai analysed the data, Guohua Fan and Wu Cai acquired funding, Wanliang Guo investigated related literature, Dongliang Hu chose the method, Guohua Fan and Wu Cai adminstrated the project, Shenghong Ju and Wu Cai supervised the project, Dongliang Hu and Manman Cui validated the results. Dongliang Hu, Manman Cui wrote the main manuscript text and Yan Liu，Duchang Zhai prepared figures and tables. All authors reviewed the manuscript.

Funding
This study was supported by the Project of State Key Laboratory of Radiation Medicine and Protection, Soochow University (GZK1202136).

Data availability
The datasets generated or analyzed during the study are available from the corresponding author on reasonable request.

Declarations

Ethics approval and consent to participate
The study was performed with approvals from the Second Affiliated Hospital of Soochow University institutional board and ethical committee (NO. JD-LK2023041-I01), and was carried out in strict accordance with the relevant guidelines for the acquisition and use of human information and specimens, and the Declaration of Helsinki. Informed consent was waived because of the retrospective nature of the study.

Consent for publication
Not applicable.

Competing interests
The authors declare no competing interests.

Author details
[1]Department of Radiology, The Second Affiliated Hospital of Soochow University, San Xiang Road No. 1055, Suzhou 215004, Jiangsu, China
[2]Department of Radiology, Children's Hospital of Soochow University, Suzhou, China
[3]Department of Radiology, Zhongda Hospital, Medical School of Southeast University, Nanjing, China

Received: 27 November 2024 / Accepted: 8 May 2025
Published online: 24 May 2025

References

1. Sagar S, Liu PP, Cooper LT, London. England). 2012;379(9817):738–47. https://doi.org/10.1016/s0140-6736(11)60648-x.
2. Shiravi AA, Ardekani A, Sheikhbahaei E, Heshmat-Ghahdarijani K. Cardiovascular complications of SARS-CoV-2 vaccines: an overview. Cardiol Therapy. 2022;11(1):13–21. https://doi.org/10.1007/s40119-021-00248-0.
3. Lee JW, Jeong YJ, Lee G, Lee NK, Lee HW, Kim JY, Choi BS, Choo KS. Predictive value of cardiac magnetic resonance Imaging-Derived myocardial strain for poor outcomes in patients with acute myocarditis. Korean J Radiol. 2017;18(4):643–54. https://doi.org/10.3348/kjr.2017.18.4.643.
4. Weinreich MA, Jabbar AY, Malguria N, Haley RW. New-Onset myocarditis in an immunocompetent adult with acute metapneumovirus infection. Case reports in medicine.2015; 2015:814269. https://doi.org/10.1155/2015/814269
5. Ferreira VM, Schulz-Menger J, Holmvang G, Kramer CM, Carbone I, Sechtem U, Kindermann I, Gutberlet M, Cooper LT, Liu P, et al. Cardiovascular magnetic resonance in nonischemic myocardial inflammation: expert recommendations. J Am Coll Cardiol. 2018;72(24):3158–76. https://doi.org/10.1016/j.jacc.2018.09.072.
6. Wang H, Zhao B, Jia H, Gao F, Zhao J, Wang C. A retrospective study: cardiac MRI of fulminant myocarditis in children-can we evaluate the short-term outcomes? PeerJ. 2016;4:e2750. https://doi.org/10.7717/peerj.2750.
7. Di Filippo S. Improving outcomes of acute myocarditis in children. Expert Rev Cardiovasc Ther. 2016;14(1):117–25. https://doi.org/10.1586/14779072.2016.1114884.
8. Messroghli DR, Moon JC, Ferreira VM, Grosse-Wortmann L, He T, Kellman P, Mascherbauer J, Nezafat R, Salerno M, Schelbert EB, et al. Clinical recommendations for cardiovascular magnetic resonance mapping of T1, T2, T2* and extracellular volume: A consensus statement by the society for cardiovascular magnetic resonance (SCMR) endorsed by the European association for cardiovascular imaging (EACVI). J Cardiovasc Magn Reson. 2017;19(1):75. https://doi.org/10.1186/s12968-017-0389-8.
9. Florian A, Ludwig A, Rösch S, Yildiz H, Sechtem U, Yilmaz A. Myocardial fibrosis imaging based on T1-mapping and extracellular volume fraction (ECV) measurement in muscular dystrophy patients: diagnostic value compared with conventional late gadolinium enhancement (LGE) imaging. Eur Heart J Cardiovasc Imaging. 2014;15(9):1004–12. https://doi.org/10.1093/ehjci/jeu050.
10. Aquaro GD, Ghebru Habtemicael Y, Camastra G, Monti L, Dellegrottaglie S, Moro C, Lanzillo C, Scatteia A, Di Roma M, Pontone G, et al. Prognostic value of repeating cardiac magnetic resonance in patients with acute myocarditis. J Am Coll Cardiol. 2019;74(20):2439–48. https://doi.org/10.1016/j.jacc.2019.08.1061.
11. Aquaro GD, Perfetti M, Camastra G, Monti L, Dellegrottaglie S, Moro C, Pepe A, Todiere G, Lanzillo C, Scatteia A, et al. Cardiac MR with late gadolinium enhancement in acute myocarditis with preserved systolic function: ITAMY study. J Am Coll Cardiol. 2017;70(16):1977–87. https://doi.org/10.1016/j.jacc.2017.08.044.
12. Blissett S, Chocron Y, Kovacina B, Afilalo J. Diagnostic and prognostic value of cardiac magnetic resonance in acute myocarditis: a systematic review and meta-analysis. Int J Cardiovasc Imaging. 2019;35(12):2221–9. https://doi.org/10.1007/s10554-019-01674-x.
13. Yang F, Wang J, Li W, Xu Y, Wan K, Zeng R, Chen Y. The prognostic value of late gadolinium enhancement in myocarditis and clinically suspected myocarditis: systematic review and meta-analysis. Eur Radiol. 2020;30(5):2616–26. https://doi.org/10.1007/s00330-019-06643-5.
14. Leiner T, Rueckert D, Suinesiaputra A, Baeßler B, Nezafat R, Išgum I, Young AA. Machine learning in cardiovascular magnetic resonance: basic concepts and applications. J Cardiovasc Magn Reson. 2019;21(1):61. https://doi.org/10.1186/s12968-019-0575-y.
15. Zhang N, Yang G, Gao Z, Xu C, Zhang Y, Shi R, Keegan J, Xu L, Zhang H, Fan Z, et al. Deep learning for diagnosis of chronic myocardial infarction on nonenhanced cardiac cine MRI. Radiology. 2019;291(3):606–17. https://doi.org/10.1148/radiol.2019182304.
16. Baessler B, Mannil M, Oebel S, Maintz D, Alkadhi H, Manka R. Subacute and chronic left ventricular myocardial Scar: accuracy of texture analysis on nonenhanced cine MR images. Radiology. 2018;286(1):103–12. https://doi.org/10.1148/radiol.2017170213.
17. Law YM, Lal AK, Chen S, Čiháková D, Cooper LT Jr., Deshpande S, Godown J, Grosse-Wortmann L, Robinson JD, Towbin JA. Diagnosis and management of myocarditis in children: A scientific statement from the American heart association. Circulation. 2021;144(6):e123–35. https://doi.org/10.1161/cir.0000000000001001.
18. Hsiao JF, Koshino Y, Bonnichsen CR, Yu Y, Miller FA Jr., Pellikka PA, Cooper LT Jr., Villarraga HR. Speckle tracking echocardiography in acute myocarditis. Int J Cardiovasc Imaging. 2013;29(2):275–84. https://doi.org/10.1007/s10554-012-0085-6.
19. Friedrich MG, Sechtem U, Schulz-Menger J, Holmvang G, Alakija P, Cooper LT, White JA, Abdel-Aty H, Gutberlet M, Prasad S, et al. Cardiovascular magnetic resonance in myocarditis: A JACC white paper. J Am Coll Cardiol. 2009;53(17):1475–87. https://doi.org/10.1016/j.jacc.2009.02.007.

20. Schultz JC, Hilliard AA, Cooper LT Jr., Rihal CS. Diagnosis and treatment of viral myocarditis. Mayo Clinic proceedings.2009; 84(11):1001–1009. https://doi.org/10.1016/s0025-6196(11)60670-8
21. Mahrholdt H, Goedecke C, Wagner A, Meinhardt G, Athanasiadis A, Vogelsberg H, Fritz P, Klingel K, Kandolf R, Sechtem U. Cardiovascular magnetic resonance assessment of human myocarditis: a comparison to histology and molecular pathology. Circulation. 2004;109(10):1250–8. https://doi.org/10.1161/01.Cir.0000118493.13323.81.
22. Caforio AL, Pankuweit S, Arbustini E, Basso C, Gimeno-Blanes J, Felix SB, Fu M, Heliö T, Heymans S, Jahns R et al. Current state of knowledge on aetiology, diagnosis, management, and therapy of myocarditis: a position statement of the European Society of Cardiology Working Group on Myocardial and Pericardial Diseases. European heart journal.2013; 34(33):2636–2648, 2648a-2648d. https://doi.org/10.1093/eurheartj/eht210
23. Magnani JW, Dec GW. Myocarditis: current trends in diagnosis and treatment. Circulation. 2006;113(6):876–90. https://doi.org/10.1161/circulationaha.105.584532.
24. Grün S, Schumm J, Greulich S, Wagner A, Schneider S, Bruder O, Kispert EM, Hill S, Ong P, Klingel K, et al. Long-term follow-up of biopsy-proven viral myocarditis: predictors of mortality and incomplete recovery. J Am Coll Cardiol. 2012;59(18):1604–15. https://doi.org/10.1016/j.jacc.2012.01.007.
25. Sachdeva S, Song X, Dham N, Heath DM, DeBiasi RL. Analysis of clinical parameters and cardiac magnetic resonance imaging as predictors of outcome in pediatric myocarditis. Am J Cardiol. 2015;115(4):499–504. https://doi.org/10.1016/j.amjcard.2014.11.029.
26. André F, Stock FT, Riffel J, Giannitsis E, Steen H, Scharhag J, Katus HA, Buss SJ. Incremental value of cardiac deformation analysis in acute myocarditis: a cardiovascular magnetic resonance imaging study. Int J Cardiovasc Imaging. 2016;32(7):1093–101. https://doi.org/10.1007/s10554-016-0878-0.
27. Schubert S, Opgen-Rhein B, Boehne M, Weigelt A, Wagner R, Müller G, Rentzsch A, Zu Knyphausen E, Fischer M, Papakostas K, et al. Severe heart failure and the need for mechanical circulatory support and heart transplantation in pediatric patients with myocarditis: results from the prospective multicenter registry MYKKE. Pediatr Transplant. 2019;23(7):e13548. https://doi.org/10.1111/petr.13548.
28. Akgül F, Er A, Ulusoy E, Çağlar A, Vuran G, Seven P, Yılmazer MM, Ağın H, Apa H. Are clinical features and cardiac biomarkers at admission related to severity in pediatric acute myocarditis? Clinical features and cardiac biomarkers in pediatric acute myocarditis. Archives De Pediatr: Organe Officiel De La Societe Francaise De Pediatr. 2022;29(5):376–80. https://doi.org/10.1016/j.arcped.2022.03.008.
29. Korosoglou G, Sagris M, André F, Steen H, Montenbruck M, Frey N, Kelle S. Systematic review and meta-analysis for the value of cardiac magnetic resonance strain to predict cardiac outcomes. Sci Rep. 2024;14(1):1094. https://doi.org/10.1038/s41598-023-50835-5.
30. Kass DA. Ventricular arterial stiffening: integrating the pathophysiology. (1524–4563 (Electronic)).
31. Rosen BD, Edvardsen T, Fau - Lai S, Lai S, Fau - Castillo E, Castillo E, Fau - Pan L, Pan L, Fau - Jerosch-Herold M, Jerosch-Herold M, Fau - Sinha S, Sinha S, Fau - Kronmal R, Kronmal R, Fau - Arnett D, Arnett D, Fau - Crouse JR 3. rd, Crouse Jr 3rd Fau - Heckbert SR. Left ventricular concentric remodeling is associated with decreased global and regional systolic function: the Multi-Ethnic study of atherosclerosis. (1524–4539 (Electronic)).
32. Awadalla M, Mahmood SS, Groarke JD, Hassan MZO, Nohria A, Rokicki A, Murphy SP, Mercaldo ND, Zhang L, Zlotoff DA, et al. Global longitudinal strain and cardiac events in patients with immune checkpoint Inhibitor-Related myocarditis. J Am Coll Cardiol. 2020;75(5):467–78. https://doi.org/10.1016/j.jacc.2019.11.049.
33. Luetkens JA, Schlesinger-Irsch U, Kuetting DL, Dabir D, Homsi R, Doerner J, Schmeel FC, Fimmers R, Sprinkart AM, Naehle CP, et al. Feature-tracking myocardial strain analysis in acute myocarditis: diagnostic value and association with myocardial oedema. Eur Radiol. 2017;27(11):4661–71. https://doi.org/10.1007/s00330-017-4854-4.
34. Buss SJ, Breuninger K, Lehrke S, Voss A, Galuschky C, Lossnitzer D, Andre F, Ehlermann P, Franke J, Taeger T, et al. Assessment of myocardial deformation with cardiac magnetic resonance strain imaging improves risk stratification in patients with dilated cardiomyopathy. Eur Heart J Cardiovasc Imaging. 2015;16(3):307–15. https://doi.org/10.1093/ehjci/jeu181.
35. Pedrizzetti G, Claus P, Kilner PJ, Nagel E. Principles of cardiovascular magnetic resonance feature tracking and echocardiographic speckle tracking for informed clinical use. J Cardiovasc Magn Reson. 2016;18(1):51. https://doi.org/10.1186/s12968-016-0269-7.
36. Amzulescu MS, De Craene M, Langet H, Pasquet A, Vancraeynest D, Pouleur AC, Vanoverschelde JL, Gerber BL. Myocardial strain imaging: review of general principles, validation, and sources of discrepancies. Eur Heart J Cardiovasc Imaging. 2019;20(6):605–19. https://doi.org/10.1093/ehjci/jez041.
37. Claus P, Omar AMS, Pedrizzetti G, Sengupta PP, Nagel E. Tissue tracking technology for assessing cardiac mechanics: principles, normal values, and clinical applications. JACC Cardiovasc Imaging. 2015;8(12):1444–60. https://doi.org/10.1016/j.jcmg.2015.11.001.
38. Nucifora G, Miani D, Di Chiara A, Piccoli G, Artico J, Puppato M, Slavich G, De Biasio M, Gasparini D, Proclemer A. Infarct-like acute myocarditis: relation between electrocardiographic findings and myocardial damage as assessed by cardiac magnetic resonance imaging. Clin Cardiol. 2013;36(3):146–52. https://doi.org/10.1002/clc.22088.

Publisher's note